Supporting Information

Atomic-scale RuS_{2-x} Clusters with Rich-defect for Efficient Electron Trap of Bacterial Respiratory Chains

*Qingshan Liu[1], Zhen Wan[1], Ruoli Zhao[2], Hao Zhang[1], Yadong Zhe[1], Jiarong Li[2], Xiaoyu Mu[1,2 *], Xiao-Dong Zhang[1,2 *]*

[1] Tianjin Key Laboratory of Brain Science and Neural Engineering, Academy of Medical Engineering and Translational Medicine, Tianjin University, Tianjin 300072, China

[2] Department of Physics and Tianjin Key Laboratory of Low Dimensional Materials Physics and Preparing Technology, School of Sciences, Tianjin University, Tianjin 300350, China

Materials and methods

Synthesis of RuS_{2-x} clusters

10.4 mg of $RuCl_3$ (Heowns, 99%) was dissolved in 20 mL of ultrapure water to prepare the Ru-precursor solution. 0.2 mL of 0.5 M Na_2S (Aladdin, > 95%) solution was then added dropwise to the 5 mL $RuCl_3$ solution under vigorous stirring at room temperature. A clear brown solution containing RuS_{2-x} clusters was formed. The RuS_{2-x} clusters were subsequently collected by centrifugation (12,000 rpm, 10 min), washed three times with ultrapure water, and dried under vacuum overnight.

Synthesis of $RuSe_2$ and $RuTe_2$ clusters

$RuSe_2$ and $RuTe_2$ clusters were synthesized following previous literature with minor modifications. To prepare Se precursors, 80 mg of $NaBH_4$ (Aladdin, > 98%) was dispersed in 1 mL of ultrapure water and 80 mg of Se powder (Heowns, > 99.9%) was added and stirred under N_2 protection. 20 min later, the black Se powder dissolved completely. Similarly, 1 mL of $NaBH_4$ solution (50 mg $NaBH_4$) was mixed with 50 mg of Te powder (Heowns, > 99.9%) under N_2 protection. After 20 min, the black Te powder disappeared. Subsequently, 0.2 mL of the Se or Te precursors solution was added dropwise to 5 mL of $RuCl_3$ solution under vigorous stirring at room temperature. After an additional 10 min stirring, the product was collected by centrifugation (12000 rpm, 10 min), washed three times with ultrapure water, and dried under vacuum overnight.

Instruments and characteristics

Transmission electron microscopy (TEM) images were captured with a JEOL JEM-2100F instrument at 200 kV. The height of RuX_2 clusters was measured by atomic force microscopy (AFM, Dimension Icon, Bruker). X-ray photoelectron spectroscopy (XPS) was performed with a Thermo Escalab 250Xi instrument. X-ray diffraction (XRD) patterns were obtained using a Rigaku Rint 2500 diffractometer, which employs monochromated Cu Kα radiation for accurate

analysis. The energy level structure of the RuX_2 clusters was determined by ultraviolet photoelectron spectroscopy (UPS, Axis Supra, Kratos Analytical Ltd, UK). Electron spin resonance (ESR) spectrum measurements were performed using an electron paramagnetic resonance spectrometer (Bruker EMX plus, Germany).

Assessment of the peroxidase-like activity

The POD-like activity of RuX_2 clusters was evaluated by monitoring the absorbance changes at 652 nm. For the colorimetric reaction, a mixture of 3,3',5,5'-tetramethylbenzidine (TMB, 0.1 mM) and H_2O_2 (50 mM) was prepared, with TMB serving as the chromogenic substrate. Then, RuX_2 clusters were incubated with the mixture, and the increase in absorbance was directly proportional to the oxidation of TMB. To further investigate the reaction dynamics of RuX_2 clusters, the Michaelis-Menten kinetic model was applied to determine the Michaelis constant (K_m) and the maximum reaction velocity (V_{max}). The Michaelis-Menten constant was calculated as following equation:

$$1/V = (K_m/V_{max})\,(1/[E] + 1/K_m)$$

The kinetic constant (K_{cat}) was calculated based on the equation:

$$K_{cat} = V_{max} / [E]$$

where V is the initial velocity, V_{max} represents the maximum reaction velocity, [E] is the concentration of substrate, and K_m corresponds to the Michaelis constant. By inverting both sides of the equation, V_{max} and K_m were determined from the corresponding double reciprocal plot.

Detection of the GSHOx-like activity and steady-state kinetic analysis

Glutathione (GSH) consumption was evaluated using Ellman's assay. Typically, 50 μL of GSH (1 mM, Heowns, 98%) was treated with four groups: control, RuS_{2-x}, $RuSe_2$, $RuTe_2$. The final working concentrations of GSH, DTNB 5,5-dithiobis (2-nitrobenzoic acid) (Heowns, 98%), and catalyst were 1 mM, 200 μg mL^{-1} and 25 μg mL^{-1}, respectively. After incubation for

20 min at 37°C, 2 μL of DTNB (20 mg mL^{-1}) was added to each group to record absorbance values at 412 nm. The steady-state kinetic was assessed with the catalyst in the presence of DTNB (200 μg mL^{-1}) and various GSH concentrations (0.05, 0.1, 0.25, 0.5, 1.0 and 2.0 mM). The absorbance was recorded by a UV-vis spectrophotometer (ε=13600 M^{-1} cm^{-1} for TNB). The Michaelis-Menten constant was determined using the Lineweaver-Burk method, $1/V = (K_m/V_{max})\ (1/[E] + 1/K_m)$. To verify the generation of hydrogen peroxide, different concentrations of RuS_{2-x} were added to the GSH solution and the absorbance at 240 nm was recorded by UV spectrophotometer.

Bacteria current detection

According to previous literature,[1, 2] the current-potential (I-V) curves were collected using a CHI660E electrochemical workstation with a 5 mM $K_3[Fe(CN)_6]$ (Heowns, > 98%) redox system. The catalyst served as the working electrode, while a platinum wire and saturated calomel electrode (SCE) as the counter electrode and reference electrode, respectively. The working electrode potential was scanned from -0.5 to 0.5 V. I-V curves were recorded both in the presence and absence of *E. coli*.

Evaluation of antibacterial activity *in vitro*

The *in vitro* antibacterial efficacy of RuX_2 clusters was assessed using the plate counting method. *Escherichia coli* (*E. coli*), *Staphylococcus aureus* (*S. aureus*), *Enterococcus faecium, Acinetobacter baumannii, Pseudomonas aeruginosa and Klebsiella Pneumoniae* were used to evaluate the broad-spectrum antimicrobial efficacy of RuX_2 clusters. Bacterial suspension (1×10^8 CFU mL^{-1}) was treated as follows: Saline, $RuTe_2$, $RuSe_2$ and RuS_{2-x}. The final concentration of clusters is 100 μg mL^{-1}. After incubation for 30 min in each group, 100 μL of each bacterial suspension was spread on the LB solid agar plate and incubated at 37 ℃ for 24 h to count the bacterial colonies.

Live-Dead bacteria staining

Initially, bacterial cells subjected to various treatments were collected via centrifugation (5000 rpm, 5 min) and washed 3 times with saline. Subsequently, the treated bacteria were stained in the dark with SYTO9 and PI (Shanghai Nonin Biological Technology Co., Ltd.) for 30 min. The green and red fluorescence intensities of various groups were observed using a confocal laser scanning microscope.

ROS level of Bacterial

The levels of reactive oxygen species (ROS) in bacteria were assessed using the fluorescent probe 2',7'-Dichlorofluorescin Diacetate (DCFH-DA, Solarbio, >97%). Bacteria were collected by centrifugation after various treatments and then incubated with DCFH-DA for 15 min under dark conditions. Subsequently, the fluorescence intensity was measured using flow cytometry.

Detection of bacterial ATP content

After treatment with RuX_2 clusters at the concentrations of 100 μg mL^{-1} for 12 h at 37 ℃, the bacterial cells were mixed with an ATP extracting solution and then disrupted using an ultrasonic processor. The treated bacterial suspensions were then centrifuged at 10000 rpm for 5 min at 4 °C. The supernatant was used to measure the ATP activity by the ATP content Assay Kit (Solarbio, China).

O-nitrophenyl-β-D-galactopyranoside (ONPG) assay

The bacterial suspension (OD600=0.5) was harvested and incubated with ONPG (25 mM) solution for 1 h. Subsequently, the supernatant was collected by centrifugation, and its absorbance was measured at 405 nm.

Fluorescence imaging

10 μL Rhodamine B (1 mg mL^{-1}) added to RuS_{2-X} (1 mg mL^{-1}), and then incubated for overnight at 200 rpm. RhB-labeled RuS_{2-x} were collected by centrifufugation and washed three times with double distilled water. The bacterial suspension (OD600=0.5) were incubated with

RhB-labeled RuX_{2-x} (100 μg mL^{-1}) 1 h. After co-incubation, the bacterial was collected and the fluorescence images were captured by fluorescence microscope.

Crystal Violet (CV) staining

200 μL of *E. coil* (OD = 0.1) was added to the 96-well plate and cultured at 37°C for 48 h to form a biofilm. Then, the mature biofilms were gently washed three times with PBS. The well plate was replaced with fresh medium containing RuX_2 clusters (100 μg mL^{-1}) or PBS and co-cultured at 37°C for another 6 h. 200 μL of CV (Solarbio, AR) solution (1%) was added to the well plate and incubated for 10 min at room temperature. The CV solution was removed and washed with DI water. The fixed dye was dissolved with 100 μL of 33% (v/v) acetic acid and incubated for 30 min at room temperature. The biomass of the biofilm was quantified by recording the absorbance at 595 nm using a microplate reader.

***In vivo* antibacterial and wound-healing experiment**

All experimental mice (BALB/c, 6-8 weeks) were purchased from Tianjin Yi Shengyuan Gene Technology Co., Ltd. All animal procedures followed the ethics and ethics rules of the Animal Committee and complying with the principles of animal protection, animal welfare and ethics (YSY-DWLL-2024545). A circular wound with a diameter of 8.0 mm was created on the back of each mouse, and 25 μL of *E.coli* suspension (10^8 CFU mL^{-1}) was placed on the wounds for constructing the infected wound model. After 24 h, the infected mice were randomly divided into four groups (n = 6): (1) Saline, (2) $RuTe_2$, (3) $RuSe_2$ and (4) RuS_{2-x}. The mice were treated on days 1, 3, 5, and 7, respectively, with daily monitoring of wound changes and mouse weights. After 10 days of treatment, the mice were sacrificed, and wound skin tissues, as well as organ tissues (heart, liver, spleen, lung and kidneys), were collected for hematoxylin-eosin (HE) staining analysis.

Cytotoxicity and biocompatibility

Cortical microvessel endothelial cells (CMEC) and macrophage cells (RAW264.7) were plated in a 96-well plate with 100 μL DMEM medium and incubated at 37 ℃. After 12 h, the cells were exposed to various concentrations of RuX_2 clusters for 24 h. Subsequently, Cell viability was assessed using a Cell Counting Kit-8 (CCK-8) assay. On day 10, blood samples were collected from the mice for biochemical analysis. Additionally, major organs were harvested after 10 days for pathological examination.

Statistical analysis

Data are presented as mean ± standard deviation (SD) or standard error of the mean (SEM). Comparison of means between two groups was accomplished by the Student's t-test. For multiple comparison, one- way analysis of variance (ANOVA) was used to assess difference in means among groups. $*P < 0.05$, $**P < 0.01$, and $***P < 0.001$, analyzed by ANOVA.

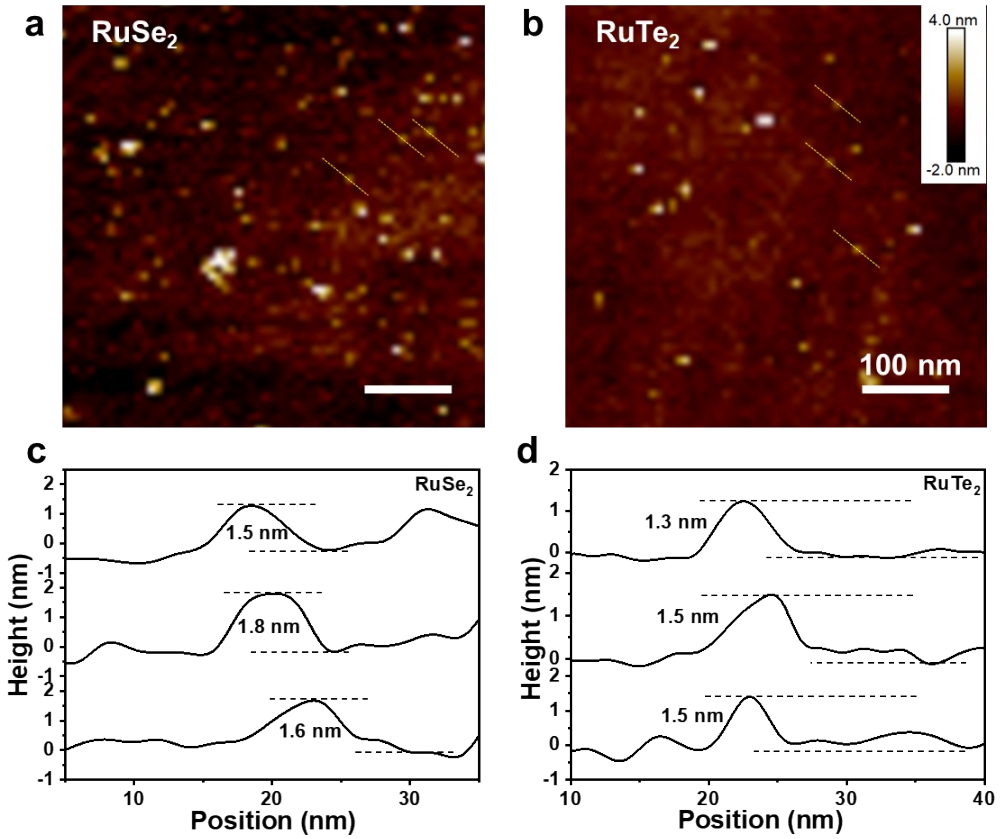

Figure S1. AFM image of (a) $RuSe_2$, (b) $RuTe_2$ clusters and the corresponding height profile (c-d).

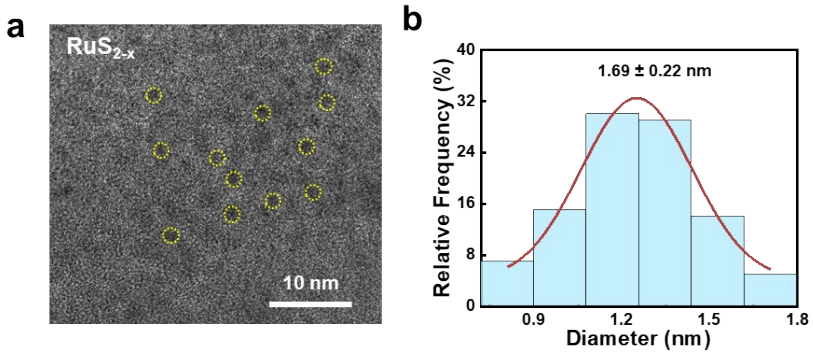

Figure S2. TEM image of (a) RuS_{2-x} and corresponding size distribution (b).

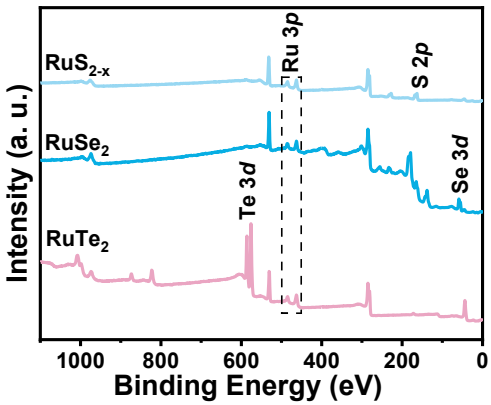

Figure S3. XPS full spectra of RuX_2 clusters.

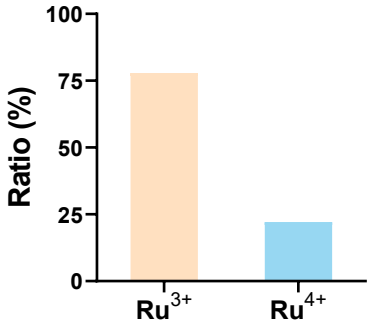

Figure S4. Ratios of Ru^{3+} and Ru^{4+} in RuS_{2-x} clusters according to XPS results.

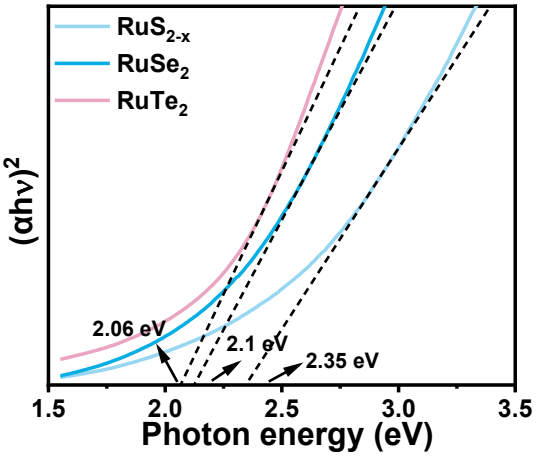

Figure S5. Plot analysis of optical bandgap of RuX_2 clusters.

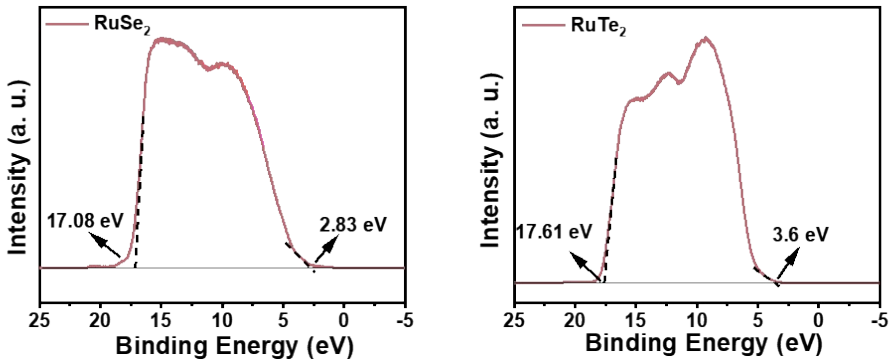

Figure S6. UPS spectra measured by He I ($h\nu$ = 21.22 eV) spectra. The secondary electron cutoff (left). The valence band (right)

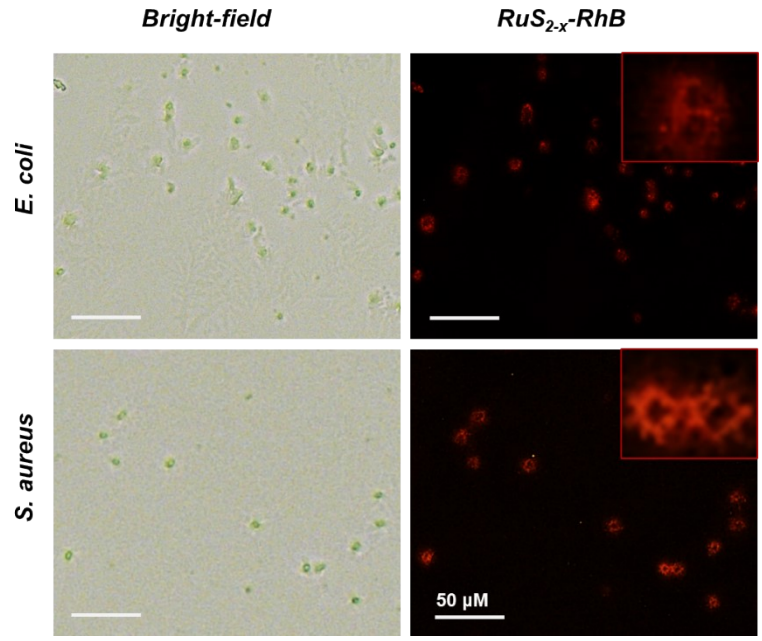

Figure S7. Fluorescent images of *E. coli* and *S. aureus* incubated with RhB-labeled RuS_{2-x}.

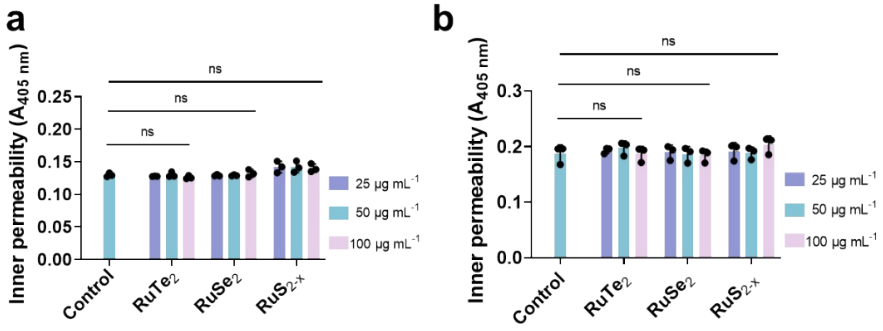

Figure S8. Permeability of bacterial membrane determined by ONPG assay analysis of *E. coli* (a) and *S. aureus* (b) after RuX_2 clusters treatments.

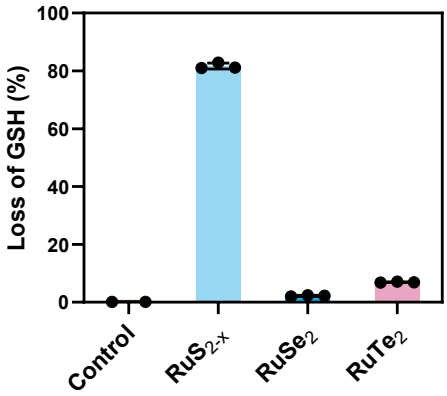

Figure S9. Quantitative analysis of GSH loss in different reaction systems.

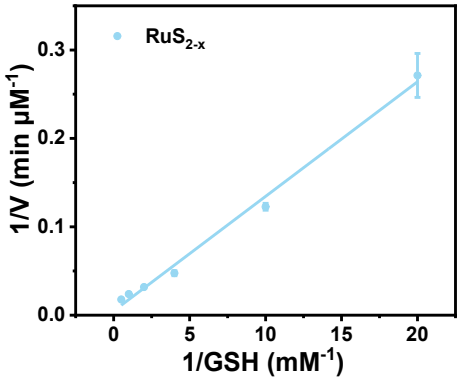

Figure S10. Double-reciprocal plots of kinetic constants for RuS_{2-x} of GSH.

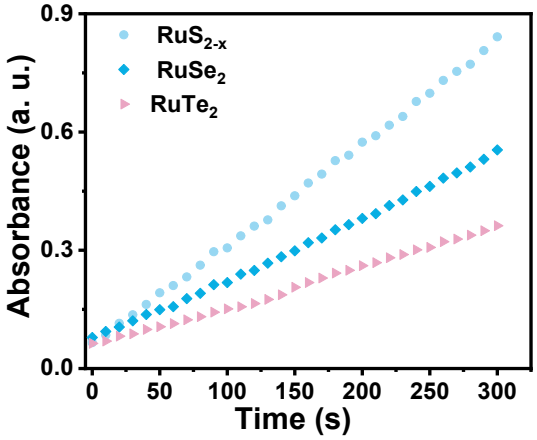

Figure S11. Time-dependent absorption changes of TMB in the presence of RuX_2 and H_2O_2.

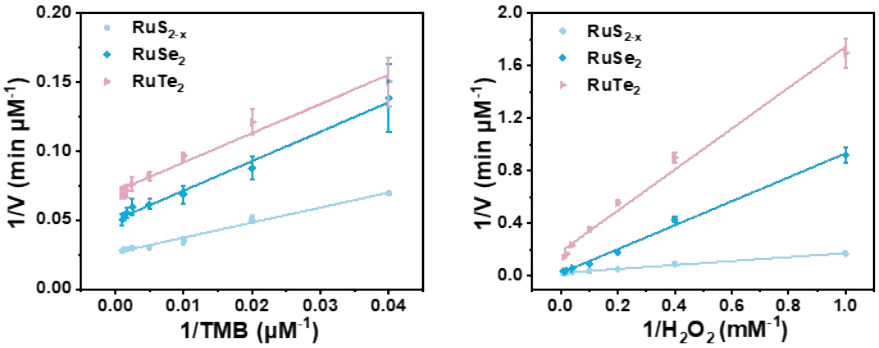

Figure S12. Double-reciprocal plots of kinetic constants for different samples of TMB and H_2O_2.

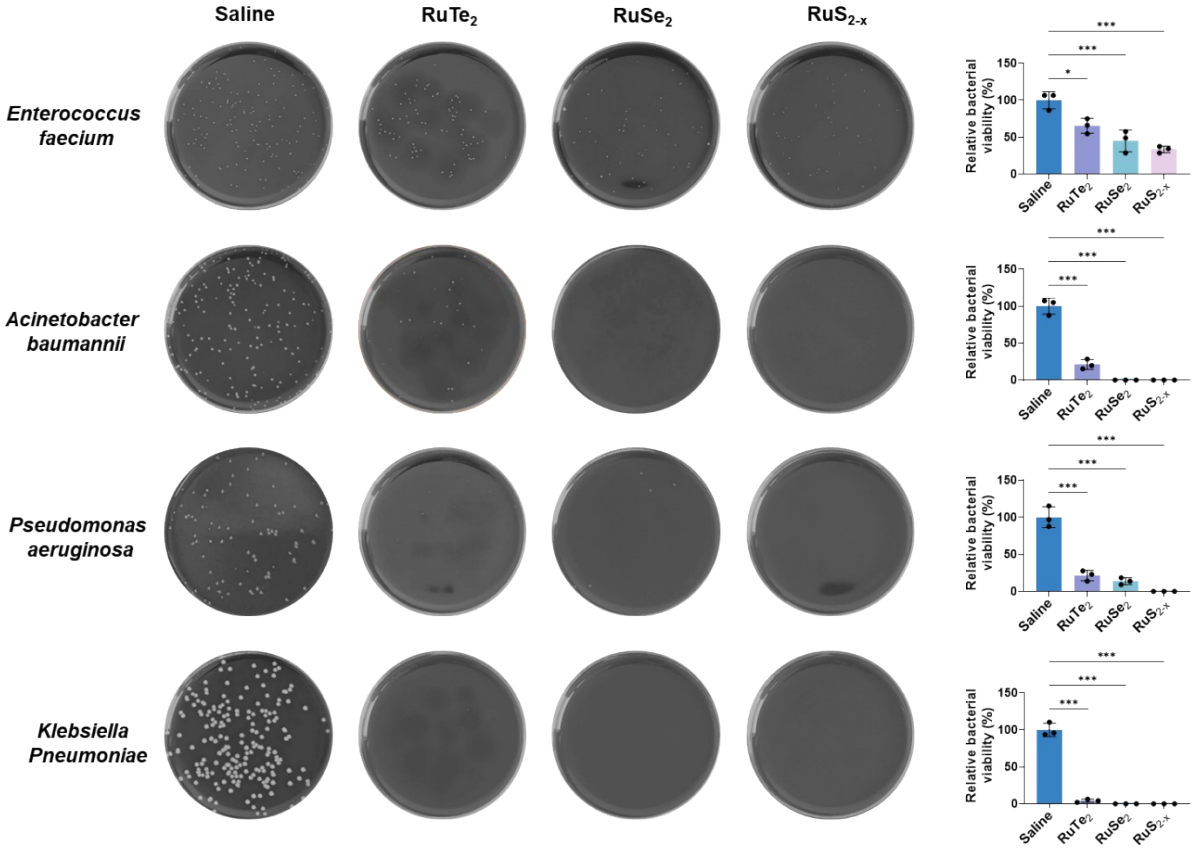

Figure S13. Representative photographs of agar plates and the relative bacterial viability of *Enterococcus faecium, Acinetobacter baumannii, Pseudomonas aeruginosa and Klebsiella Pneumoniae* with RuX_2 clusters treatments.

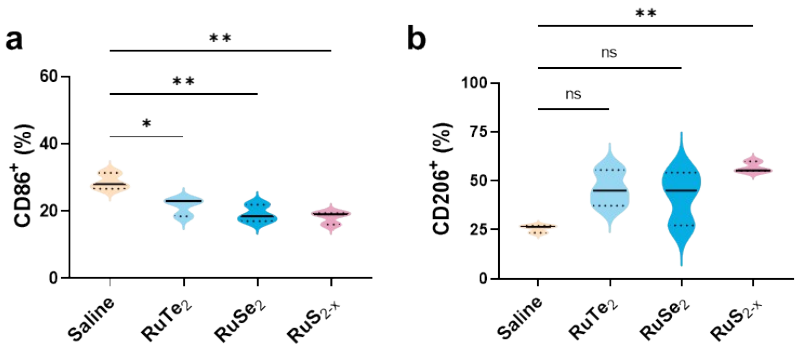

Figure S14. Statistical analysis of (a) CD86, (b) CD206 content after different treatments. n=3 per group. Data are presented mean ± SEM; *$p < 0.05$, **$p < 0.01$, and ***$p < 0.001$ versus with the control group, analyzed by ANOVA.

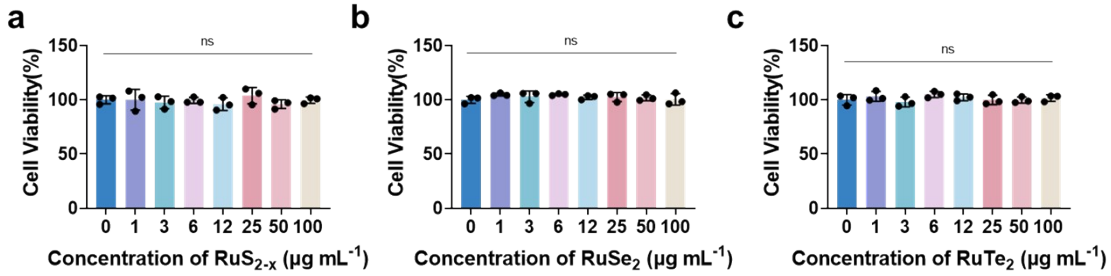

Figure S15. Cytotoxicity of different concentrations of RuS_{2-x} clusters on macrophage cells (RAW264.7). n=3 per group. Data are presented mean ± SEM; *$p < 0.05$, **$p < 0.01$, and ***$p < 0.001$ versus with the control group, analyzed by ANOVA.

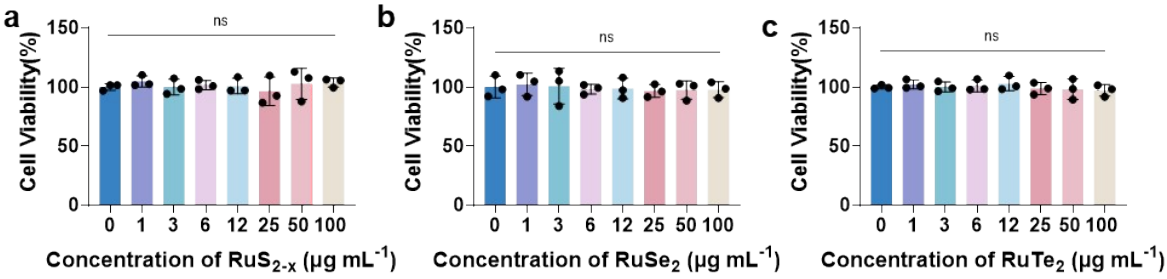

Figure S16. *In vitro* cytotoxicity of the RuX_2 clusters on cortical microvessel endothelial cells. n=3 per group. Data are presented mean ± SEM; *$p < 0.05$, **$p < 0.01$, and ***$p < 0.001$ versus with the control group, analyzed by ANOVA.

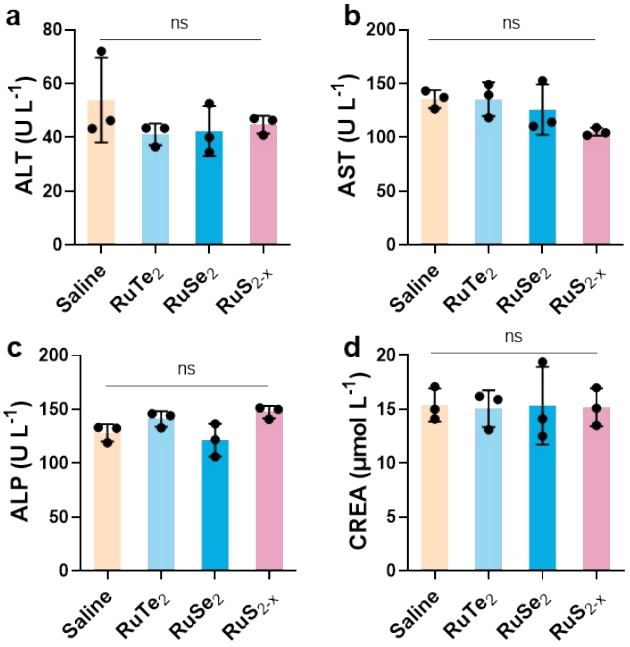

Figure S17. Levels of different blood biochemistry indexes with various treatments after 10 days. The results show mean and standard error of the mean of alanine aminotransferase (ALT), aspartate aminotransferase (AST), alkaline phosphatase (ALP) and creatinine (CREA), n=3 per group. Data are presented mean ± SEM; *$p < 0.05$, **$p < 0.01$, and ***$p < 0.001$ versus with the control group, analyzed by ANOVA.

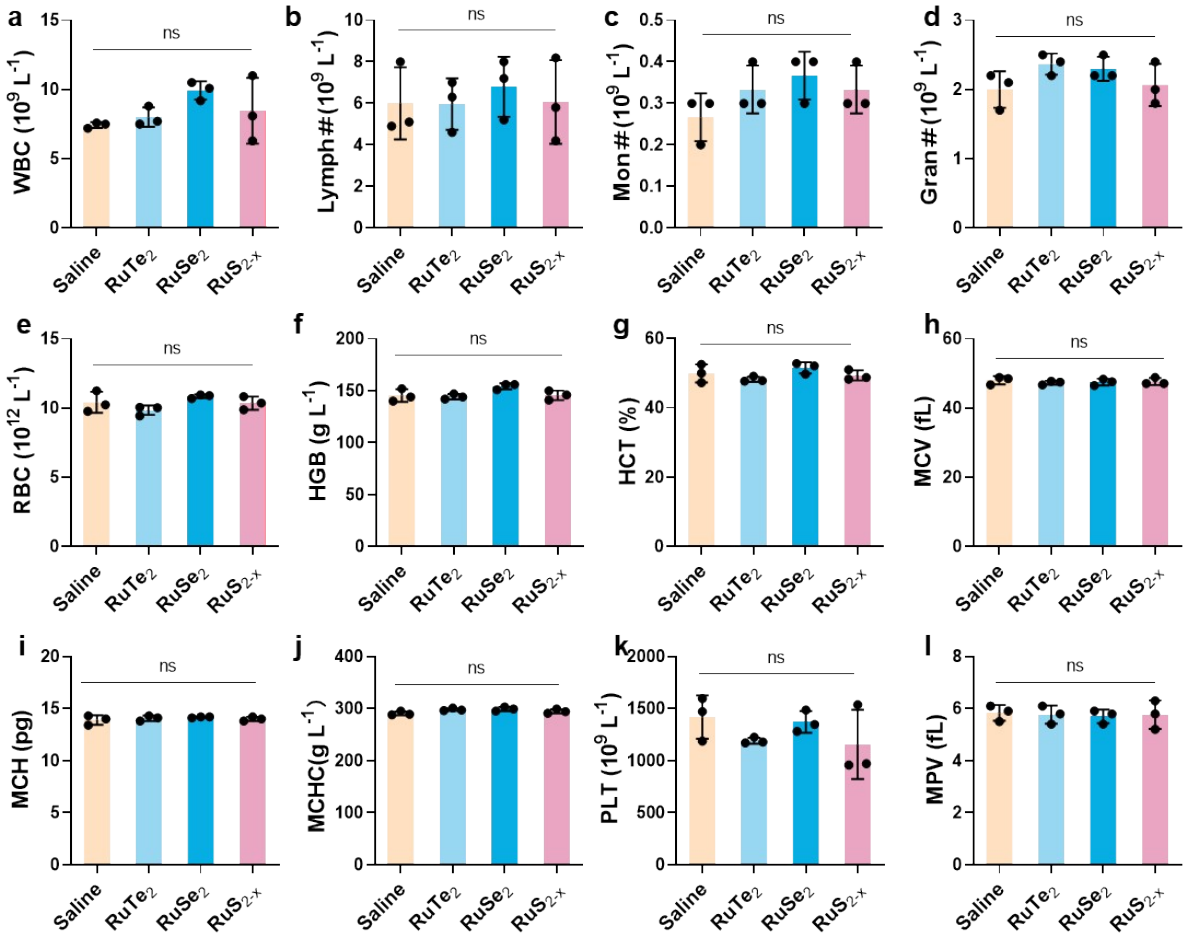

Figure S18. Levels of different blood routine indexes with various treatments after 10 days. The results show the mean and standard error of the mean of white blood cells (WBC), lymphocyte (Lymph), monocyte (Mon), granulocyte (Gran), red blood cell (RBC), hemoglobin (HGB), hematocrit (HCT), mean corpuscular volume (MCV), mean corpuscular hemoglobin (MCH), mean corpuscular hemoglobin concentration (MCHC), platelets (PLT), and mean platelet volume (MPV), n=3 per group. Data are presented as mean ± SEM; $*p < 0.05$, $**p < 0.01$, and $***p < 0.001$ versus the Sham group, analyzed by ANOVA.

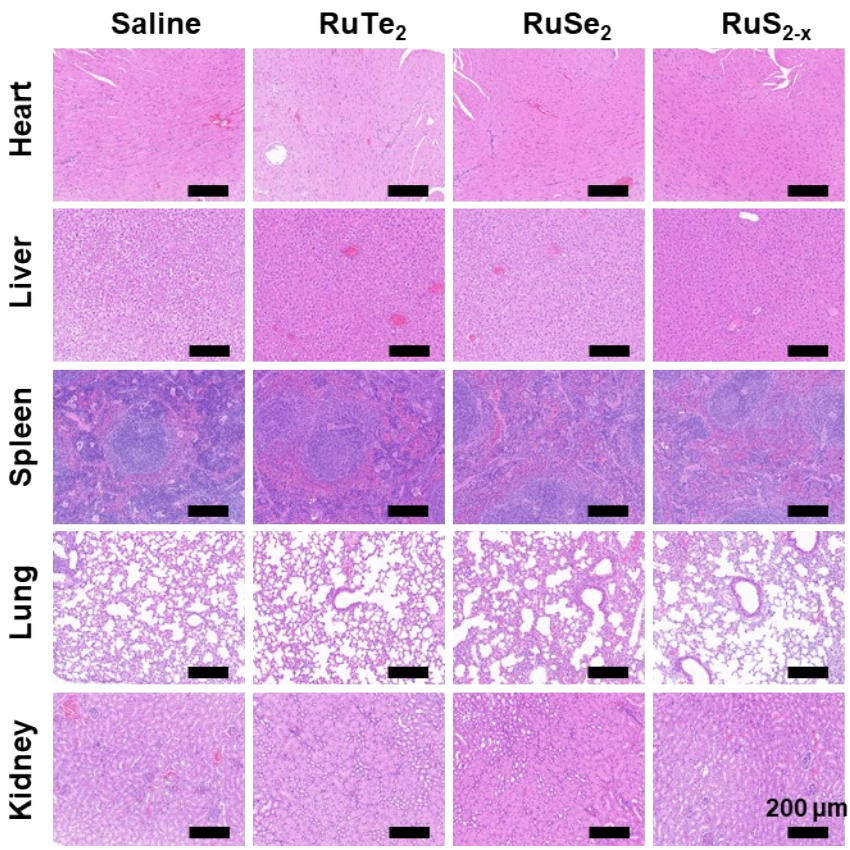

Figure S19. Histotoxicological assessment of major organs (heart, spleen, liver and kidney) stained with hematoxylin and eosin (H&E) after 10 days of different treatments. Scale bar is 200 μm, n=3 per group. No significant toxic responses were found in all organs.

Table S1. Kinetic parameters for the GSHOx-like activity of different samples

Samples	*[E]* (M)	K_m (mM)	V_{max} (μM min^{-1})	K_{cat} (min^{-1})	References
Cu-N_4	1.72×10^{-6}	0.288	33.9	19.7	[3]
Cu-NS	1.51×10^{-6}	0.33	51.12	37.8	[3]
Fe_3O_4	2.02×10^{-7}	0.53	3.97	19.7	[4]
Fe-N_4	2.73×10^{-9}	0.13	36.42	13300	[4]
Zn-NC	5.42×10^{-5}	1.3	1.63	0.03	[5]
Ga-NC	3.70×10^{-6}	0.89	1.76	0.474	[5]
Ga/Zn-NC	2.78×10^{-6}	0.58	13.14	4.74	[5]
Pd Sazyme	6.77×10^{-6}	0.24	1182	175	[6]
S-N/Ni PSAE	3.27×10^{-6}	0.83	6720	2060	[7]
MnSA-N_3-C	-	0.3	120	4240	[8]
MnSA-N_4-C	-	0.43	85.8	2590	[8]
Fe-N-C	3.21×10^{-6}	3.11	1674	512	[9]
Fe-S/N-C	2.59×10^{-6}	1	20760	8020	[9]
RuS_{2-x}	6.69×10^{-10}	0.75	76.52	114000	This work

Table S2. Comparison of kinetic parameters for HRP and RuX_2 clusters.

Samples	[*S*] (M)	Substrates	K_m (mM)	V_{max} (μM min^{-1})	K_{cat} (min^{-1})	K_{cat}/K_m (mM min^{-1})
RuS_{2-x}	5.35×10^{-10}	TMB	0.36	37.38	6.98×10^4	1.94×10^5
		H_2O_2	9.20	51.76	9.67×10^4	1.05×10^4
$RuSe_2$	8.00×10^{-10}	TMB	0.38	19.75	2.47×10^4	6.50×10^4
		H_2O_2	25.41	35.63	4.45×10^4	1.75×10^3
$RuTe_2$	1.28×10^{-9}	TMB	0.39	14.67	1.15×10^4	2.94×10^4
		H_2O_2	33.38	10.98	8.58×10^4	2.57×10^2
HRP		TMB	0.552	0.13	1.63×10^4	2.95×10^4
		H_2O_2	1.56	0.08	1×10^4	6.41×10^4

1. J. Guo, X. Pan, C. Wang, Z. Huang, Z. Huang, J. Deng, Q. Wu, Y. Sun, X. Xu, D. Hou and H. Liu, *Adv. Mater.*, **2025**, e06721.
2. G. Wang, H. Feng, A. Gao, Q. Hao, W. Jin, X. Peng, W. Li, G. Wu and P. K. Chu, *ACS Appl. Mater. Interfaces*, **2016**, *8*, 24509-24516.
3. R. Niu, Y. Liu, B. Xu, R. Deng, S. Zhou, Y. Cao, W. Li, H. Zhang, H. Zheng, S. Song, Y. Wang and H. Zhang, *Adv. Mater.*, **2024**, *36*, 2312124.
4. X. Zhu, J. Wu, R. Liu, H. Xiang, W. Zhang, Q. Chang, S. Wang, R. Jiang, F. Zhao, Q. Li, L. Huang, L. Yan and Y. Zhao, *ACS Nano*, **2022**, *16*, 18849-18862.
5. S. Zhong, Z. Zhang, Z. Wang, Q. Zhao, W. Chen, G. Chen, Z. Jiang, Q. Cai, L. Gong, Y. Lai, D. Wang and L. Li, *J. Am. Chem. Soc.*, **2025**, *147*, 15814-15826.
6. M. Chang, Z. Hou, M. Wang, C. Yang, R. Wang, F. Li, D. Liu, T. Peng, C. Li and J. Lin, *Angew. Chem., Int. Ed.*, **2021**, *60*, 12971-12979.
7. Y. Zhu, W. Wang, P. Gong, Y. Zhao, Y. Pan, J. Zou, R. Ao, J. Wang, H. Cai, H. Huang, M. Yu, H. Wang, L. Lin, X. Chen and Y. Wu, *ACS Nano*, **2023**, *17*, 3064-3076.
8. Y. Wang, A. Cho, G. Jia, X. Cui, J. Shin, I. Nam, K.-J. Noh, B. J. Park, R. Huang and J. W. Han, *Angew. Chem., Int. Ed.*, **2023**, *62*, e202300119.
9. W. Liu, Q. Chen, J. Wu, F. Zhang, L. Han, J. Liu, H. Zhang, Z. Hao, E. Shi, Y. Sun, R. Zhang, Y. Wang and L. Zhang, *Adv. Funct. Mater.*, **2024**, *34*, 2312308.